Sea-level rise and coastal vulnerability: an assessment of Andhra Pradesh coast, India through remote sensing and GIS

K. Nageswara Rao · P. Subraelu ·
T. Venkateswara Rao · B. Hema Malini · R. Ratheesh ·
S. Bhattacharya · A. S. Rajawat · Ajai

Abstract The eustatic sea-level rise due to global warming is predicted to be about 18 to 59 cm by the 2100 (IPCC 2007), which necessitates identification and protection of vulnerable sections of coasts. Assessment of vulnerability level of Andhra Pradesh (AP) coast as an example is demonstrated in this study using five physical variables, namely coastal geomorphology, coastal slope, shoreline change, mean spring tide range, and significant wave height. A coastal vulnerability index was prepared by integrating the differentially weighted rank values of the five variables, based on which the coastline is segmented into low-, moderate-, high-, and very high risk categories. About 43% of the 1,030-km-long AP coast is under very high-risk, followed by another 35% under high-risk if the sea level rises by ~0.6 m displacing more than 1.29 million people living within 2.0 m elevation in 282 villages in the region.

Keywords Sea-level rise · Coastal vulnerability index · Coastal risk assessment · Andhra Pradesh coast

K. Nageswara Rao (✉) · P. Subraelu · T. Venkateswara Rao
Department of Geo-Engineering, Andhra University,
Visakhapatnam 530 003, India
e-mail: nrkakani@yahoo.com

B. Hema Malini
Department of Geography, Andhra University,
Visakhapatnam 530 003, India

R. Ratheesh · S. Bhattacharya · A. S. Rajawat · Ajai
Marine and Earth Sciences Group, Space Applications Centre,
Ahmedabad 380 015, India

Introduction

The global average temperature is increasing over the past century. It is generally believed that the Earth warmed from ~1900 to 1940, cooled slightly from ~1940 to 1965–1970 and then warmed markedly from ~1970 onward (Hansen et al. 2001; Trenberth et al. 2007). While the global warming in the past century was estimated to be 0.8°C, the rise in temperature in the past three decades alone was 0.6°C at the rate of 0.2°C per decade as greenhouse gases became the dominant climate forcing in recent decades (Hansen et al. 2006; IPCC 2007; Rosenzweig et al. 2008; Wood 2008). Even the reported cooling of global temperature from 1940 to 1970 is now considered due to instrumental bias in the sea surface temperature record occurred around that time (Thompson et al. 2008). The ramifications of global warming both in physical and biological world, by and large, reflect the impact of greenhouse gases (Rosenzweig et al. 2008; Zwiers and Hegerl 2008). Arctic ice sheet is rapidly retreating and if this trend continues the polar bear population would decrease by two-thirds by the mid-century (Courtland 2008). Comparing the altitudinal distribution of 171 forest plant species between 1905 and 1985, and 1986 and 2005 along the entire elevation range up to 2,600 m above sea level, Lenoir et al. (2008) observed that the climate warming has resulted in a significant upward shift in species optimum elevation averaging 29 m per decade. The warming is also worsening the public health problems such as the alarming spread of malaria in Africa and elsewhere, and the increasing risk of respiratory diseases and metabolic disorders owing to poor air quality and rising temperatures (Hoyle 2008). Even the steep

increase in food prices that are currently witnessed all over the world is probably the first genuinely global effects of greenhouse gas warming, as the demand for supplies is aggravated by the drought in food-producing regions (Parry et al. 2008).

Perhaps the most commonly recognized impact of global warming is the eustatic rise in sea level (Allen and Komar 2006) due to thermal expansion of seawater and addition of ice-melt water (Meehl et al. 2005). Already there are evidences of large-scale ice melt in the three major ice repositories of the world. The Greenland ice is melting at a rate of 239 ± 23 km^3 per year (Chen et al. 2006). The extent of Arctic sea ice has been decreasing at almost 8% per decade since the middle of last century (Stroeve et al. 2007). Based on a recent space-borne radar and LIDAR study, Kay et al. (2008) found that in 2007 the cloud cover over the Arctic decreased by 16% than in the previous year which allowed radiation influx leading to melting of about 0.3-m-thick surface ice. The summer-time shrinkage of Arctic sea ice in August 2007 was at an unprecedented 31% lower than the long-term average and the lowest extent in the satellite record for any month (NSIDC 2007). Perhaps the most alarming is the widespread loss of ice in West Antarctica (Rignot et al. 2008) contributing to global sea-level rise of ~0.36 mm/year (Chen et al. 2008). On the whole, the climate change-induced rise in global sea level is estimated to be 1–3 mm/year (Pielke et al. 2007). Even if the global temperatures are leveled off at this stage, the sea level continues to rise over the 21 century (Meehl et al. 2005). IPCC (2007) predicted that the global sea level will rise by at most 59 cm by 2100. However, many feel that there are inconsistencies in the IPCC estimates (Pielke 2008; Pielke et al. 2008; Schiermeier 2008). A more recent estimate based on a new model allowing accurate construction of sea levels over the past 2,000 years suggest that the melting of glaciers, disappearing of ice sheets and warming water could lift the sea level by as much as 1.5 m by the end of this century (Strohecker 2008). The direct impact of the sea-level rise is on the coastal zones which, in spite of being highly resourceful and densely populated, are low-lying and hence would be subjected to accelerated erosion and shoreline retreat due to increased wave strength as water depth increases near the shore (Pirazzoli 1996; Pye and Blott 2006), besides leading to saltwater intrusion into coastal groundwater aquifers, inundation of wetlands and estuaries, and threatening historic and cultural resources as well as infrastructure (Pendleton et al. 2004). The increased sea-surface temperature would also result in frequent and intensified cyclonic activity and associated storm surges affecting the coastal zones (Unnikrishnan et al. 2006; Wu et al. 2002).

The rising sea level endangers several smaller island nations, such as Tuvalu, Maldives, etc., which are barely 2 m above the sea level (Brown 2001). Millions of people in low-lying regions of many other countries including Bangladesh, China (Strohecker 2008), and Vietnam (Tanh and Furukawa 2007) face the danger of being displaced. In this background, identifying the vulnerability of different coastal sectors to the impact of the rising sea levels is an important aspect of coastal zone management. Quantification is needed to determine the degree of vulnerability experienced by a coast (Sanchez-Arcilla 1998) since measuring vulnerability is a key step towards effective risk reduction (Birkmann 2006). Many attempts have been made to measure coastal vulnerability and estimate risk intensities to sea-level rise taking various physical variables such as coastal landforms, relief, geology, relative sea-level changes, history of shoreline change, tide and wave regimes, etc. (Diez et al. 2007; Doukakis 2005; Gornitz 1991; Pendleton et al. 2004; Thieler and Hammer-Klose 1999) mainly from USA, Europe, Brazil, etc.

There are indications that sea-levels are increasing along the east coast of India too. Studies based on the analysis of long-term tide-gauge data from various stations along the Indian coastal regions, corrections for vertical land movements included, indicated that sea levels are rising at a rate of about 1.0–1.75 mm per year due to global warming (Unnikrishnan et al. 2006; Unnikrishnan and Shankar 2007). Although this estimate is based on too much of generalization considering the fact that the tide-gauge stations with long-term data are too few along the Indian coasts, the indications of sea-level rise, however, are obvious. Pronounced erosion even along certain major depocentres like deltas of the east coast of India although was mainly attributed to anthropogenic forcing (e.g. Baskaran 2004; Hema Malini and Nageswara Rao 2004; Nageswara Rao et al. 2008), perhaps reflect the impact of sea-level rise as well among other things such as coastal subsidence. But there are hardly any studies on coastal vulnerability assessment of the Indian coasts. The purpose of this paper is to quantitatively assess the degree of vulnerability of various coastal sectors of Andhra Pradesh state along the east coast of India to the impending sea-level rise.

Study area

The east coast of India bordering the Bay of Bengal is a passive continental margin developed during separation of India from Antarctica in the Late Jurassic (Bastia and Nayak 2006). Administratively, the 2,350-km-long east coast forms the eastern seaboard of three States—Orissa in the north, Andhra Pradesh (AP) in the centre, and Tamil Nadu in the south. The present study area is the 1,030-km-long coast of AP State including the 300-km-long Krishna–Godavari delta front dominating its central part (Fig. 1).

The coastal sector north of these deltas is characterized by headland-bay configuration with a number of rock promontories jutting into the sea, especially over a 185-km stretch on both sides of Visakhapatnam city (inset B in Fig. 1). The Penner delta and Pulicat Lake (the second largest lagoon along the east coast after Chilika Lake in Orissa) are the dominant features along the coast south of the Krishna–Godavari delta region. The region is densely populated with more than 6.5 million people (2001 census) living within 5-m-elevation above the sea level including the port cities of Visakhapatnam, Kakinada and Machilipatnam. The AP coast is known for frequent tropical cyclones and associated floods and tidal surges causing loss of life and property in the region. For example, the 1977 cyclone that was accompanied by a 5-m storm surge killed about 10,000 people and 0.2 million livestock besides
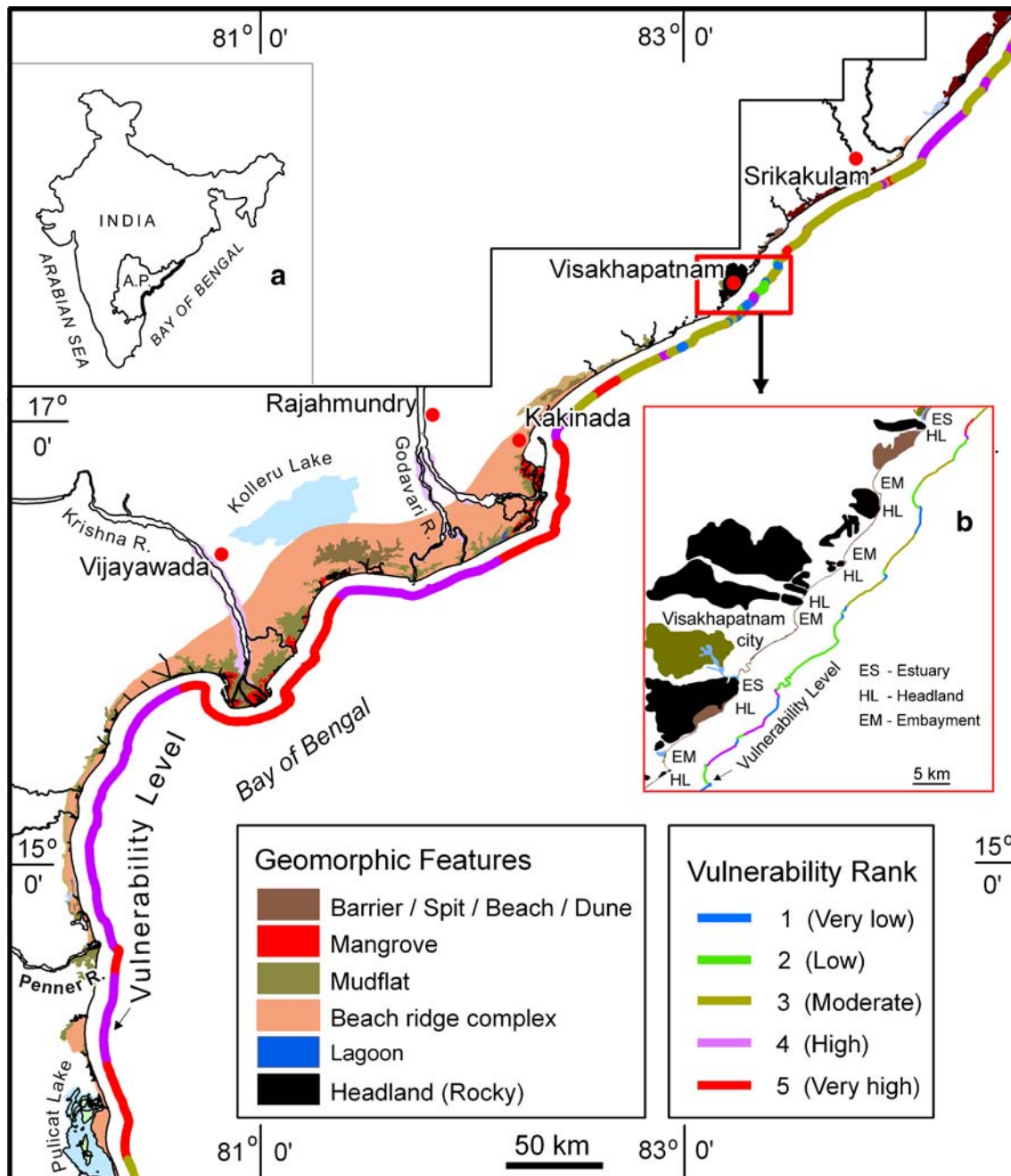
Fig. 1 Geomorphology of the AP coast up to ~5 m elevation (except at the rock headlands). Inset **a** shows the outline of AP State in India with AP coast shown as a *thick black line*. Inset **b** shows the headland-bay configuration of the coast on both sides of Visakhapatnam city in an enlarged format. The thick colored parallel line all along the AP coast (including in the inset **b** as well), indicates the vulnerability ranking of various segments of the AP coast based on the relative resistance of the geomorphic features that fringe the coast

causing enormous damage to property in the Krishna delta region. The 3- to 4-m storm surges occurred respectively in the 1990 and 1996 killed thousands of people and millions of livestock, besides damaging property in Godavari delta region. The 1999 super cyclone and associated 7- to 8-m-high storm surge (Lal 2001; Nayak et al. 2001) killed more than 10,000 people and devastated the Mahanadi delta region in the northern state of Orissa along the east coast. The future sea-level rise is likely to further intensify the storm surges (Pendleton et al. 2004), besides accelerating shoreline erosion and other problems like seawater intrusion and damage to coastal structures, thereby making the AP coast much more vulnerable in future. The AP coast is also prone to tsunamis. The recent 2004-tsunami that caused 283,000 deaths in the coastal zones of many countries around the Indian Ocean (Lay et al. 2005), also affected the east coast of India. Although the coast of the southern state of Tamil Nadu was the most affected with tsunami inundation limits exceeding 800 m at some places (Chadha et al. 2005) killing about 10,000 people, the tsunami impacted the AP coast as well leading to loss of life and property at several locations, especially in the low-lying zones along the Krishna–Godavari deltas (Nageswara Rao et al. 2007). In this background, a coastal vulnerability assessment is made in this study aimed at identifying the degree of vulnerability of different coastal segments of AP.

Methods of study

Five physical variables of the AP coast are used in this study to measure the coastal vulnerability. They are (1) coastal geomorphology, (2) coastal slope, (3) shoreline change (erosion and accretion during a 16-year period between 1990 and 2006), (4) mean spring tide range, and (5) significant wave height. Earlier studies elsewhere considered some more parameters also for estimating the coastal vulnerability. For instance, Pendleton et al. (2004); Thieler and Hammer-Klose (1999) included relative sea-level rise as a sixth parameter besides the five listed above in the vulnerability calculations for a part of the Californian coast. Doukakis (2005) considered subsidence as one of the variables. Since there are no data either on the variations in relative sea-level rise or subsidence rates, these are not included in the present study. Gornitz (1991), Diez et al. (2007) included elevation (instead of slope), geology and sea-level rise (including the effect of local tectonics) as three of the total seven variables in their respective studies. Geology is not used as a separate variable in our study since the landform material is taken care of in geomorphology, and for the reasons mentioned above, sea-level rise is not considered a variable in our study. We consider slope a better parameter than elevation in this type of analysis, since elevation refers to a point, whereas slope,

which is calculated based on elevations and distances involved, denotes an area. Relative ranking is assigned to various coastal segments based on the vulnerability level in terms of each of the five parameters considered in the study. As such, the entire AP coast is divided into five vulnerability classes—very low, low, moderate, high, and very high, separately for each of the five variables with slight modifications to the ranking system adopted in earlier studies referred (Diez et al. 2007; Doukakis 2005; Gornitz 1991; Pendleton et al. 2004; Thieler and Hammer-Klose 1999).

Physical variables and their ranking

As stated already, five physical variables are considered in this study for a quantitative assessment of the vulnerability of AP coast to the predicted sea-level rise. They are (1) Coastal geomorphology, (2) Coastal slope, (3) Shoreline change during the recent years, (4) Mean spring tide range, and (5) Significant wave height. Depending up on the nature of each of these variables, the entire AP coast is segmented and assigned vulnerability ranks ranging from 1 to 5, with rank 1 representing very low vulnerability and rank 5 indicating very high vulnerability as detailed in the following sections.

Geomorphology (g)

Morphology of the coast plays an important role in determining the impact of sea-level rise. Landforms and the material that compose them reflect their relative responses to sea-level rise since every landform offers certain degree of resistance to erosion (Thieler and Hammer-Klose 1999). While the rocky cliffs and wave-cut benches offer maximum resistance and therefore very less vulnerable, the soft sandy and muddy forms such as dunes, mudflats, mangroves, etc., that offer least resistance, on the other hand, are extremely vulnerable to sea-level rise. A detailed geomorphic map (Fig. 1) showing the various coastal landforms is prepared in this study based on the interpretation of satellite images (Indian Remote Sensing Satellite—IRS P6 Advanced Wide Field Sensor data from the 2006) substantiated by field observations during the last 2 years. The AP coast like the entire east coast of India is predominated by depositional landforms such as beach ridge-swale complexes, mangrove swamps, mudflats, spits, barriers, lagoons, estuaries, and tidal inlets except in a few localities on both sides of Visakhapatnam city where a number of rocky headlands are fringed by cliffs, wave-cut benches, sea stacks and other related erosional landforms (inset **b** in Fig. 1) as noted in some previous studies as well (Nageswara Rao and Sadakata

1993; Nageswara Rao et al. 2005). The Krishna–Godavari twin deltas in the central parts, and the Penner delta and Pulicat Lake to the south along the AP coast are very low-lying as evident from landforms like beaches, mudflats, mangrove swamps, and tidal channels/creeks that spread up to more than 10–15 km inland even in this microtidal environment. The normal spring high tide reaches up to about 35 km upstream in the distributary courses of Krishna and Godavari rivers up to the maximum Holocene transgression limit, which is marked by the landward limit of the beach ridges, i.e., former shorelines (Nageswara Rao and Sadakata 1993). Considering the nature of landforms qualitatively, the entire AP coast is segmented into five vulnerability classes as per the classification scheme detailed in Table 1. Following this scheme, a vulnerability rank number is assigned to each segment of the coast (indicating the vulnerability level in terms of the geomorphology of the coast) as depicted in Fig. 1 for further analysis in geographic information system (GIS).

Coastal slope (s)

Coastal slope is the major factor to be considered along with the coastal morphology in estimating the impact of sea-level rise on a given coast. On a steep coast, the impact of sea-level rise would be insignificant contrary to a gently sloping coast where any rise in sea level would inundate large extents of land. The major constraint in our study is lack of fine resolution contour maps of the area. The Survey of India (SOI) topographic maps show 10-m contour interval in 1:25,000 scale which are of no use since most of the area of study is far below 10 m, expect at the rocky headlands near Visakhapatnam. The digital elevation models (DEM) of the AP coastal area available on the internet from the Shuttle Radar Topographic Mission (SRTM) website (www.srtm.csi-cgiar.org) are downloaded from which contours at 1-m interval are interpolated using the *3-D Analyst* module in ArcGIS software. But when the contour map thus generated was overlaid on the landform

map, many inconsistencies were noticed owing to the coarse resolution (90 m) of the SRTM data. For example, the tidally submergible mudflats are enclosed by a 4-m contour at a number of locations like in Godavari delta, although such landforms are well within 2-m elevation along the AP coast where the maximum normal spring high tide is about 1.5 m above the datum. Further, the contours appear to cross certain coastal water bodies like lagoons and backwater zones, which is not realistic. Therefore, extensive corrections were made to bring in accuracy in the contours taking into consideration the nature of landforms (from satellite imagery), and spot heights and tidal limits as can be noted from the SOI topographic maps. Using the '*Edit*' mode in ArcMAP for this purpose, the contour layer was overlaid on satellite images and topographic maps alternately while the contours are adjusted. Firstly, the innermost beach-ridge all along the AP coast, which runs at different distances inland from the present shoreline from a few hundred meters to even up to 35 km, as in the Krishna–Godavari delta region, is taken as 5-m contour. Similarly, the high-tide line which is either marked in the SOI topographic maps or interpreted in this study based on the landward limit of mangrove swamps and active tidal mudflats, is taken as 1.5 m line because the maximum mean spring high-tide anywhere along AP coast is 1.5 m on an average as can be noted from the hydrographic charts. Therefore, all the intertidal areas along AP coast fall between the shoreline and the 1.5-m contour in the map. A 0.6 m contour is also interpolated between the shoreline (0-m contour) and the 1.5 m contour. This is meant to represent the approximate limit of the IPCC (2007) predicted sea-level rise of 0.59 m by the end of the 2100. Beach ridges which are at various elevations from 2 m up to 5 m in the AP coast are taken into consideration while interpolating the contours all along the AP coast. The contours thus generated are used to prepare a slope map for the AP coast through triangulated irregular network (TIN) method in 3-D Analyst module of ArcGIS. The slope values ranged from 0.00485% to 1.2177%. The entire range

Table 1 Coastal vulnerability classification based on the five physical variables

Variable	Coastal vulnerability rank				
	Very low (1)	Low (2)	Moderate (3)	High (4)	Very high (5)
Geomorphology	Rocky coasts	Embayed/indented coasts	Beach ridges; high dunes (>3m) vegetated	Low fore dunes (<3m); Estuaries; lagoons	Mudflats; Mangroves; Beaches; Barriers/Spits
Coastal slope (%)	>1.00	0.50–1.00	0.10–0.50	0.05–0.10	<0.05
Shoreline change (m/year)	Accretion >5.0	Accretion <5.0	Nil	Erosion <5.0	Erosion >5.0
Mean spring tide range (m)	<1.0	1.0–2.0	2.0–4.0	4.0–6.0	>6.0
Significant wave height (m)	<0.55	0.55–0.85	0.85–1.05	1.05–1.25	>1.25

of slopes is categorized into five rank classes from 1 to 5 keeping in view the fact that higher the slope value, lower the vulnerability of the coast. The five vulnerability classes and the slope range in each class are adopted from Pendleton et al. (2004) as shown in Table 1. Based on this, vulnerability ranks (indicating the vulnerability levels in terms of coastal slope) are assigned to all segments of the coast, as shown in Fig. 2a for further GIS analysis.

Shoreline Change (c)

The broad trends in shoreline behavior in the recent past are helpful to a certain extent in understanding the coastal response to future sea-level rise. The geomorphological and land use maps in digital form that were prepared earlier based on the interpretation of satellite images (IRS 1B Linear Imaging Self Scanning Sensor 2) pertaining to the year 1990 are used to make comparison with the present (2006) coastline map. By using the overlay technique in GIS, the shift in shoreline during the 16-year period from 1990 to 2006 is extracted. As the resultant map (Fig. 2b) shows, the shoreline shifted landward due to erosion at a number of locations over a combined length of 424 km accounting for a loss of 93 km^2 coastal area. Shoreline advanced into the sea due to accretion at several locations including certain deltaic sectors as well. The total land gained by accretion is about 57 km^2 over a length of about 266 km. The remaining 340-km-long coast has not shown any notable change during the period. Considering the rate of change, which was variable along the coast, vulnerability ranking is assigned to various coastal segments following the ranges in the ranking scheme given in Table 1. Applying this classification, all the coastal sectors along the AP coast are ranked from one to five as depicted in Fig. 2b, for further analysis.
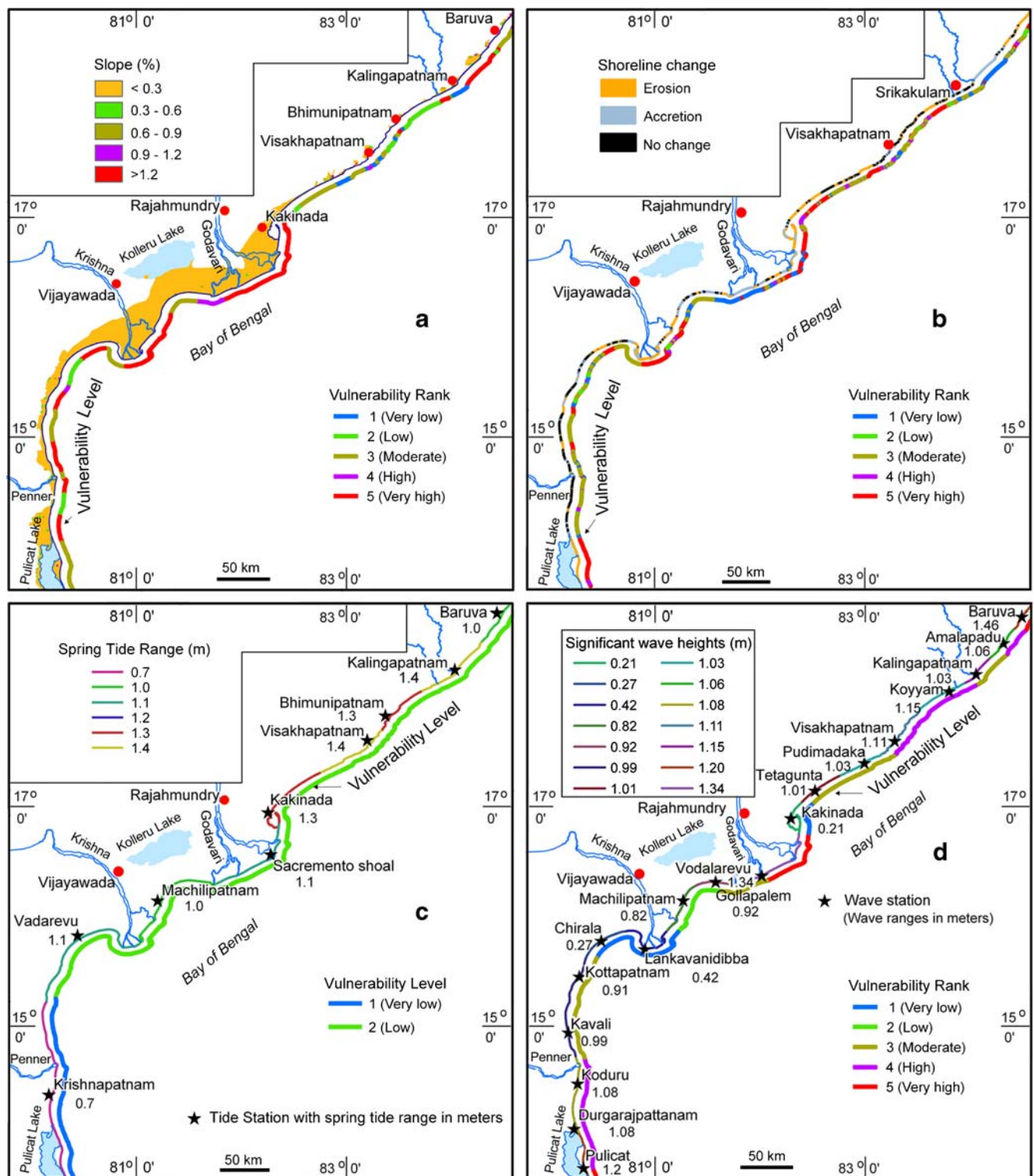
Spring-tide range (t)

As can be seen from the tidal ranges shown in the hydrographic charts published by the Indian National Hydrographic Office, the AP coast is under the influence of a microtidal environment. The mean spring tide range (the average of spring high- and low-tides) is taken into consideration from 9 stations all along the coast (Fig. 2c). The spring-tide range at Krishnapatnam in the south is the lowest at 0.7 m, whereas the highest range of 1.4 m is at Visakhapatnam in the northern sector of the AP coast (where the spring high tide is 1.5 m and the spring low tide is 0.1 m above the datum). Based on the tidal ranges at these 9 points, the entire coastline is segmented to assign the tide range value of the nearest tide station. For instance, the coastline between Krishnapatnam (0.7 m) and Vadarevu (1.1 m) to its immediate north is divided into 2 equal segments with the segment near Krishnapatnam represent-

ing the tidal range of 0.7 m, while the segment near Vadarevu representing the tidal range of 1.1 m. Similarly, the coastline between Vadarevu (1.1 m) and Machilipatnam (1.0 m) is segmented into two equal parts to represent 1.1 m near Vadarevu and 1.0 m near Machilipatnam. Thus, the entire AP coastline is segmented based on the tidal range values at the 9 stations. Subsequently, the vulnerability ranking is given (Table 1) following the vulnerability ranges from Diez et al. (2007). Since the tidal range is between 0.7 m and 1.4 m, the entire AP coast has fallen into two categories only, namely very low vulnerable level (<1.0 m) and low vulnerable level (1.0 to 2.0 m) as far as the tidal range is considered. Accordingly, the entire coast is classified into these two vulnerability categories as shown in Fig. 2c.

Significant wave height (w)

In the absence of in situ wave data for the AP coast, computer simulated wave models are used in this study. The Spectral Wave (SW) model of MIKE-21, a software developed by the Danish Hydraulic Institute, Denmark was used for simulation of the waves. Wind velocity component derived from ECMWF (European Center for Medium Range Weather Forecast) assimilated with near real-time measurements through Seawinds scatterometer onboard QuikSCAT satellite and by the three Special Sensor Microwave Imager (SSM/I) onboard DMSP (Defense Meteorological Satellite Program) satellites F13, F14, and F15, which are available from the CERSAT (Centre ERS d'Archivage et de Traitement— *French ERS Processing and Archiving Facility*) website (ftp://ftp.ifremer.fr/ifremer/cersat/products/gridded/mwf-blended/data/) were input into the model for generating the waves. The model simulates the growth, decay and transformation of wind-generated waves and swells in offshore and coastal areas (Vethamony et al. 2006).

The data on the significant wave heights (SWH) pertaining to July and August 2005 thus derived from the simulation model for the Machilipatnam region were compared for accuracy with the measured data of the corresponding period from the buoy DS5 of NIOT (National Institute of Ocean Technology) moored off Machilipatnam. A correlation coefficient of 0.873 with an RMS of 0.41 m was obtained from the comparison between the two data sets indicating the dependability of the simulated wave data. Therefore, the simulated SWH data are extracted for 19 stations (Fig. 2d) covering the entire AP coast. In order to assign the SWH values to the entire coast, the coastal segment between two consecutive wave stations is divided into two equal parts and the SWH value of the nearest station is assigned to each coastal division. Further, considering the SWH values of different coastal sections, the entire AP coast is classified into five vulnerability levels (Fig. 2d) adopting the SWH ranges

Fig. 2 Map showing the four physical variables of **a** coastal slope, **b** coastal change during the 16-year period between 1990 and 2006, **c** mean spring-tide range, and **d** significant wave heights along the AP coast. The thick colored parallel line all along the coast indicates the vulnerability ranking of the various segments based on the respective physical variable mapped

(Table 1) from Pendleton et al. (2004), and Thieler and Hammer-Klose (1999).

Coastal vulnerability index

All the five maps showing the coastline segmented according to their vulnerability ranks are then combined in GIS to derive a coastal vulnerability index (CVI) for various segments of the entire coast. The CVI was calculated by Diez et al. (2007), Doukakis (2005), Gornitz (1991), and Thieler and Hammer-Klose (1999) as the square root of the product of the ranking factors (1 to 5 for each parameter) divided by the number of parameters considered. Gornitz (1991) opined that although the CVI can be computed as either the sum or product of the parameters, the latter has the advantage of expanding the range of values. Diez et al. (2007), on the other hand, by examining both the sum as well as the product of all the variables, observed that the CVI as the sum of differentially weighted variables was more responsive to the environmental diversity. Our calculations using both the methods also indicated that the sum of the five variables with the rank numbers (1 to 5) of each multiplied by a specified weightage value, as detailed below, represents the conditions along the AP coast better. As such, the five variables are differentially weighted by multiplying the vulnerability rank values by certain arbitrarily chosen multiplication factors depending up on the relative significance of the five variables considered in the study.

For instance, geomorphology and the slope of the coast are the two major factors influencing the coastal response to sea-level rise. This was amply evident from the impact of the killer tsunami that occurred on December 26, 2004. Several studies made along the east coast of India indicated the role of geomorphology and coastal slope in tsunami impact. Ramanamurthy et al. (2005) observed that the worst affected Nagapattinam area in the southern state of Tamil Nadu along the east coast of India had longer penetration of tsunami inland due to gentle slope of the coastland. Chadha et al. (2005) noted that the coastal morphology made large difference in loss of life as the low swales behind shore-parallel dune ridges claimed several lives due to lateral flows from tidal inlets or breaches in dune ridges. Banerjee (2005) observed that the landforms of the coastal zone have relation with tsunami devastation. The overall inundation limit decreased from south to north in the state of Tamil Nadu, from the maximum of about 800 m in the southern part to about 160 m in the northern parts (Chadha et al. 2005). However, the tsunami inundation limit has significantly increased again to 700–800 m much further northward in the Krishna–Godavari delta region in the central part of AP state, where about 100 deaths were also reported, owing to

extremely gentle slope of the area (Nageswara Rao et al. 2007). Therefore, considering the relative significance of geomorphology and slope over the rest of the three variables in deciding the coastal response to sea-level rise, a maximum weightage of 4 is assigned to these two variables. Accordingly, the rank values of both these variables are multiplied by four for the CVI calculation. The third variable 'shoreline change' is assigned a weightage value of 2. The rate of shoreline change in the past cannot be taken as a constant for predicting the future behavior of the coast but is only a general indicator of the trend. Therefore, only a one half of the weightage value given to the first two variables is assigned to this variable. As such the vulnerability rank numbers of all the segments of AP coast in respect of the variable, *shoreline change* are multiplied by two for the CVI calculation. The rank numbers representing the tide range and significant wave height are taken for calculation without assigning any additional weightages. Thus, the weighted values of all the five variables are used to calculate the CVI for the entire AP coast through the process of addition using the following formula:

$$\text{CVI} = 4g + 4s + 2c + t + w$$

Where g refers to vulnerability ranking of geomorphology of the coastal segment in question, s refers to that of coastal slope, c to that of shoreline change, t refers to spring tide-range and w refers to the vulnerability rank of the significant wave height. The numbers 4 and 2 are the arbitrary weightage factors assigned to the respective variables depending up on their relative significance. The data are processed in geographic information system software (we used ArcGIS). Each variable in the form of a '*Shape File*' is taken into GIS and the vulnerability ranks of all the coastal segments for the five variables are entered into the corresponding attribute tables against the unique ID of each coastal segment. Similarly, the weighted values of each variable for each coastal segment are also obtained by multiplying the vulnerability rank values by the corresponding weightage factors of the respective variables. For example, if the vulnerability rank of a particular coastal segment is 5 (i.e., very high vulnerable) for the variable 'geomorphology', the rank value 5 is multiplied by the weightage factor of 4, which is assigned to geomorphology. Therefore, the weighted value for that coastal segment would be 20 as far as geomorphology is concerned. Likewise the weighted values of all the coastal segments for all the variables are entered in the corresponding column in the attribute tables. In fact, the computer automatically generated the weighted values once the formula with the multiplication factor is given in the corresponding column head in the attribute table. Then the shape files are joined using the '*Spatial Join*' option in '*Overlay*' module in '*ArcTools*' menu. In order to integrate all

the variables, we have taken the coastline as a line feature in GIS, whereas in earlier studies the coast was divided into spatial grids of 1-min interval (Pendleton et al. 2004), 15-min interval (Diez et al. 2007), or as closely spaced points along the coast (Doukakis 2005). However, such grid cell, or point sampling would have some amount of generalization thereby affecting the accuracy of the final results. Therefore, we have taken the entire coast as a line feature in GIS in which every point along the coast is considered for the analysis. The final output map contains the attributes of all the five variables. Thus the final map generated combining all the variables showed 307 segments of the coast each having a unique identity number in its corresponding attribute table. Another column is added to this attribute table for the CVI formula so that the system generated the CVI values for all the 307 coastal segments of the AP coast by adding the weighted values of the vulnerability ranks assigned to the various segments of all the five variables.

The CVI values thus obtained ranged from 15 to 57. The entire range of CVI values can be divided into four equal parts (Diez et al. 2007; Gornitz 1991), quartiles (Pendleton et al. 2004) or percentiles (Doukakis 2005) each indicating certain risk level of the coastline to sea-level rise. The lower range of CVI values indicate low-risk, followed by moderate-risk, high-risk and finally the upper range of values indicating the coast at very high-risk level. We tested these methods. The CVI values when divided into four equal parts, only the rocky coasts along the AP coast have fallen into the low risk coasts. However, in the quartile/ percentile methods even the sand dune coasts also come under the low-risk category. But a comparison of the geomorphology map (Fig. 1) and the shoreline change map (Fig. 2b) show wide-spread erosion along certain dune-front coastal sectors like along the Pulicat Lake coast, which cannot be classified as low-risk coast. Therefore, we divided the entire range of CVI values (15 to 57) into four equal parts in this study. Accordingly, the coastal risk level map for the AP coast is generated by grouping various coastal segments into the four risk classes (Fig. 3).

Discussion

The risk classification indicates that 43% of the AP coast over a length of 442.4 km is under the very high-risk category mostly along the Krishna, Godavari and Penner delta front coastal sectors (Fig. 3), which are very low-lying and almost flat with mudflats, mangrove swamps, and lagoons/backwaters. Moreover, these coastal sections are experiencing sustained erosion for the last three decades. Even the small tidal range in these areas can reach far inland since the gradient is extremely gentle. Similarly, about 363.7-km-long coastal segments which account for 35% of the total

length are under high-risk category mostly in the southern part of the AP coast near Pulicat Lake; north of Penner delta; south of Krishna delta; and between Krishna and Godavari deltas in the central part of AP coast where the landforms and slopes although are of moderate category, the high rate of shoreline erosion and comparatively stronger wave energy make the coast high-risk prone. In the remaining part, 193.9-km-long coast (19% of the total) mainly the non-deltaic dune-front sections, come under moderate-risk category, while the rocky coast on both sides of Visakhapatnam and some embayed/indented sectors over a combined length of 30 km (3%) are in the low-risk category.

The overall CVI map showing the risk levels of different coastal segments of AP can be scaled up to any degree of enlargement in its original GIS format. But considering the scale of the Survey of India (SOI) topographic maps that are used as base maps for registering the satellite imagery from which data on landforms (geomorphology), coastal slopes and shoreline change are extracted, the CVI maps may best be used up to 1:50,000 scale. Therefore, the map grid representing the standard SOI topographic maps (1:50,000 scale) is superimposed on the CVI map to extract locality-wise risk level of the coast as detailed in Table 2. The central sector of the AP coast, i.e., the Krishna–Godavari delta region is the most vulnerable with almost two-thirds of the total length of the coast in the very high-risk category, while the rest of the coast is also within the immediate next level of high-risk category. Notably, no part of the Krishna–Godavari delta coast is in the low or moderate risk levels. Perhaps the rapid coastal retreat and habitat loss due to wide-spread erosion during the recent years in most parts of this otherwise major depocenter along the AP coast is an indication of the manifestation of the impact of the rising sea levels in the area. The southern sector of the AP coast shows more or less similar conditions with a one-half of the total length of 285.8 km in this sector is in the very high-risk category (Table 2). The northern sector however has at least 30-km-long part of the coast under low risk level due to the presence of number of rock headlands.

If the sea level rises by 0.59 m as predicted by IPCC (2007), an area of about 565 km^2 would be submerged under the new low-tide level along the entire AP coast of which 150 km^2 would be in the Krishna–Godavari delta region alone. This is estimated by superimposing the contour map (generated as explained in section on 'coastal slope') over the satellite imagery to extract the area between the zero contour (shoreline) and the 0.6 m contour. The new spring high tide reaches further inland by another ~0.6 m above its present level of 1.5 m, i.e., up to 2.1 m. In such a case, an additional area of about 1,233 km^2 along the AP coast including 894 km^2 in the Krishna and Godavari delta region alone would go under the new intertidal zone thereby directly displacing about 1.29 million people (according to
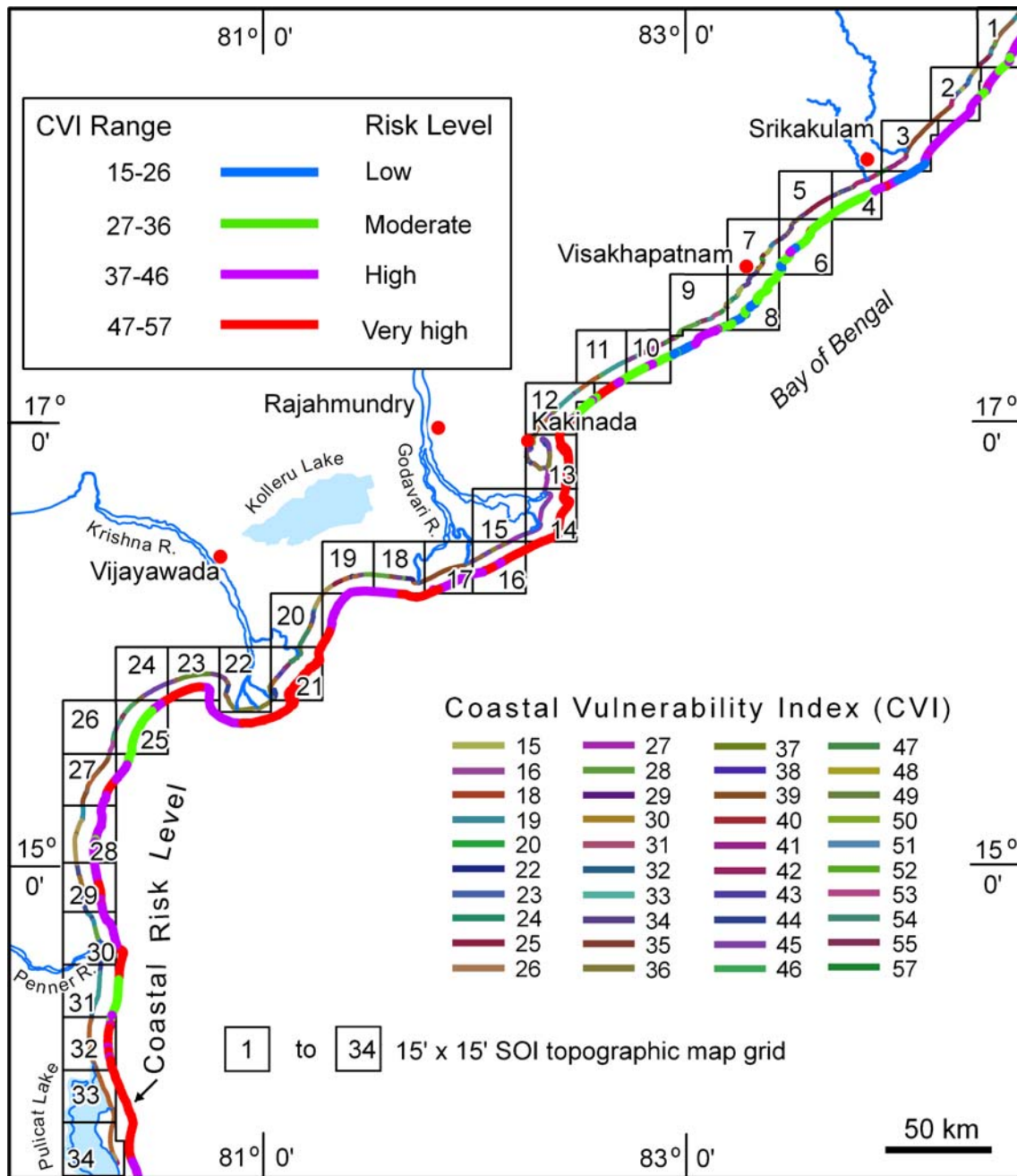
Fig. 3 Coastal vulnerability index (CVI) and risk levels of different segments of AP coast. Each color of the coastline indicates a particular CVI value from 15 to 57 (Note there are no coastal segments with CVI values of 17, 21 and 56). The *thick colored parallel line* all along the coast shows the risk levels of the coast based on the categorization of CVI values into four risk classes as per the classification scheme shown in the *upper left legend*. The *black colored squares* along the coastline (from 1 to 34) represent the grid of SOI topographic maps. The actual map IDs and the risk level of the coast covered by each map are detailed in Table 2

2001 census) who live in 282 villages spread over nine coastal districts of Andhra Pradesh state. Notably, the inhabitants of these villages are mainly hut-dwelling fishing communities who are highly vulnerable in socio-economic terms as well. Further, there is every possibility of increased storm surges (Unnikrishnan et al 2006) reaching much inland than at present with the rise in sea level.

Conclusions

In the light of the rising sea levels, assessment of coastal vulnerability is necessary in order to take appropriate measures to protect the people and property. The CVI developed for the AP coast in this study by ranking five physical variables such as coastal geomorphology, coastal

Table 2 Data on risk level of the coast in various localities represented by SOI maps in the three major sectors of the AP coast

S no.	Coastal sector	Map number	Locality	Length of the coast in each risk category (km)				
				Low	Moderate	High	Very high	Total
1	Northern Sector	74B/9	Baruva	–	1.9	32.8	2.1	36.8
2	(Visakhapatnam region)	74B/6 and 10	Naupada	–	4.9	32.9	0.9	38.7
3		74B/3	Vamsadhara estuary	5.7	11.0	22.3	2.2	41.2
4		65N/16	Nagavali estuary	–	13.3	12.5	3.8	29.6
5		65N/12	Konada	–	7.8	14.7	3.0	25.5
6		65O/9	Mukkam	–	11.4	–	–	11.4
7		65O/5	Vizag-Bhimili coast	4.0	16.0	5.2	1.4	26.6
8		65O/6	Visakhapatnam city	6.9	14.3	–	–	21.2
9		65O/2 and 3	Gangavaram	5.8	14.0	14.8	–	34.6
10		65K/15	Sarada-Varaha estuary	1.7	22.3	7.8	–	31.8
11		65K/11	Tandava estuary	–	14.8	1.2	7.7	23.7
12		65K/8 and 12	Uppada coast	5.9	10.4	6.5	17.0	39.8
Total				30	142.1	150.7	38.1	360.9
13	Central Sector	65L/5	Kakinada	–		11.8	61.7	73.5
14	(Krishna–Godavari	65L/6	Nilarevu estuary	–	–	–	31.5	31.5
15	delta region)	65L/2	Pandi lagoon	–	–	–	11.4	11.4
16		65L/3	Surasaniyanam	–	–	4.3	14.6	18.9
17		65H/15	Vainateyam estuary	–	–	22.6	5.9	28.5
18		65H/11	Vasishta estuary	–	–	18.5	10.3	28.8
19		65H/7	Goguleru creek	–	–	22.4	9.0	31.4
20		65H/4	Manginapudi	–	–	9.9	18.8	28.7
21		66E/1 and 2	Krishna estuary (Divi)	–	–	–	60.2	60.2
22		66A/13 and 14	Krishna estuary (main)	–	–	11.9	30.1	42
23		66A/11	Nizampatnam	–	–	23.9	4.5	28.4
Total						125.3	258	383.3
24	Southern Sector	66A/5	Vadarevu	–	–	3.4	15.9	19.3
25	(Penner Delta and	66A/6	Ramperu estuary	–	15.4	2.9	–	18.3
26	1Pulicat Lake region)	66A/2	Gudlakamma estuary	–	12.8	1.3		14.1
27		66A/3	Palleru-Musi estuary	–	2.7	17.8	12.9	33.4
28		66A/4	Manneru estuary	–	0.08	27.4	–	27.4
29		66B/1	Upputeru estuary	–	–	2.6	26.1	28.7
30		66B/2	Penner estuary	–	–	22.6	19.7	42.3
31		66B/3	Krishnapatnam	–	20.9	0.2	7.2	28.3
32		66B/4	Swarnamukhi estuary	–	–	4.6	23.7	28.3
33		66C/1	Durgarajpattnam	–	–	–	23.9	23.9
34		66C/2 and 6	Sriharikota island	–	–	4.9	16.9	21.8
Total				–	51.8	87.7	146.3	285.8
Grand total				30	193.9	363.7	442.4	1030

slope, rate of shoreline change, mean spring tide range and significant wave height indicated the risk level of different segments of the coast. Instead of segmenting the coast into spatial grids which might generalize the conditions to different degrees (depending up on the size of the grid cell), analyzing the entire coastline as a line feature using GIS, as demonstrated in this study, provides a more accurate picture of the vulnerability level of any point along the coast. The CVI analysis revealed that about 43% of the AP coast is under very high-risk and 35% more under high-risk, which calls for protective measures to prevent loss of invaluable coastal land and displacement of people who, mostly being hut-dwelling seafaring community are socio-economically vulnerable as well. Objective coastal vulnerability assess-

ments of this type are necessary for a proper coastal zone management. It may be noted that the maps generated in this study are scalable to any degree of enlargement in their original GIS format for application purposes.

References

Allen JC, Komar PD (2006) Climate controls on US west coast erosion processes. J Coast Res 22:511–529 doi:10.2112/03-0108.1

Banerjee A (2005) Tsunami deaths. Curr Sci 88:1358

Baskaran R (2004) Coastal erosion. Curr Sci 86:25

Bastia R, Nayak PK (2006) Tectonostratigraphy and depositional patterns in Krishna offshore basin, Bay of Bengal. Lead Edge (Tulsa Okla) 25:839–845 doi:10.1190/1.2221361

Birkmann J (2006) Measuring vulnerability to promote disaster-resilient societies: conceptual frameworks and definitions. In: Birkmann J (ed) Measuring Vulnerability to Natural Hazards. U N Univ Press, Tokyo, pp 9–54

Brown LR (2001) Rising sea level forcing evacuation of island country. Earth Policy Inst. Available via http://www.earth-policy.org/Updates/Update2.htm. Accessed on 2 Aug 2008

Chadha RK, Latha G, Yeh H et al (2005) The tsunami of the great Sumatra earthquake of *M*.9.0 on 26 December 2004—impact on the east coast of India. Curr Sci 88:1297–1301

Chen JL, Wilson CR, Tapley BD (2006) Satellite gravity measurements confirm accelerated melting of Greenland ice sheet. Science 313:1958–1960 doi:10.1126/science.1129007

Chen JL, Wilson CR, Tapley BD et al (2008) Antarctic regional ice loss rates from GRACE. Earth Planet Sci Lett 266:140–148 doi:10.1016/j.epsl.2007.10.057

Courtland R (2008) Polar bear numbers set to fall. Nature 453:432–433 doi:10.1038/453432a

Diez PG, Perillo GME, Piccolo MC (2007) Vulnerability to sea-level rise on the coast of Buenos Aires province. J Coast Res 23:119–126 doi:10.2112/04-0205.1

Doukakis E (2005) Coastal vulnerability and risk parameters. Eur Water 11/12:3–7

Gornitz V (1991) Global coastal hazards from future sea level rise. Palaeogeogr Palaeoclimatol Palaeoecol 89:379–398 doi:10.1016/0031-0182(91)90173-O

Hansen J, Ruedy R, Sato M et al (2001) A closer look at United States and global surface temperature change. J Geophys Res 106:23947–23963 doi:10.1029/2001JD000354

Hansen J, Sato M, Ruedy R et al (2006) Global temperature change. Proc Natl Acad Sci USA 103:14288–14293 doi:10.1073/pnas.0606291103

Hema Malini B, Nageswara Rao K (2004) Coastal erosion and habitat loss along the Godavari delta front – a fallout of dam construction (?). Curr Sci 87:1232–1236

Hoyle B (2008) Accounting for climate ills. Nature reports climate change. doi:10.1038/climate.2008.43

IPCC Summary for Policymakers. In: Soloman SD, Manning QM, Chen Z, Miller HL (ed) Climate Change 2007: the Physical Science Basis. Contribution of Working Group I to the Fourth Assessment Report of the Intergovernmental Panel on Climate Change Cambridge University Press, Cambridge pp 1–18.

Kay JE, L'Ecuyer T, Gettelman A et al (2008) The contribution of cloud and radiation anomalies to the 2007 Arctic sea ice extent minimum. Geophys Res Lett 35:L08503 doi:10. 1029/2008GL033451

Lal M (2001) Tropical cyclones in a warmer world. Curr Sci 80:1103–1104

Lay T, Kanamori H, Ammon CJ et al (2005) The Great Sumatra-Andaman Earthquake of 26 December 2004. Science 308:1127–1133 doi:10.1126/science.1112250

Lenoir J, Gegout JC, Marquet PA et al (2008) A significant upward shift in plant species optimum elevation during the 20th century. Scientist 320:1768–1771

Meehl GA, Washington WM, Collins WD et al (2005) How much more global warming and sea level rise. Science 307:1769–1772 doi:10.1126/science.1106663

Nageswara Rao K, Sadakata N (1993) Holocene evolution of deltas on the east coast of India. In: Kay R (ed) Deltas of the World. ASCE, New York, pp 1–15

Nageswara Rao K, Sadakata N, Hema Malini B, Takayasu K (2005) Sedimentation processes and asymmetric development of the Godavari delta, India, In: Gioson L, Bhattacharya JP (ed). River Deltas. SEPM Spl Publ 83:435–451

Nageswara Rao K, Ashokvardhan D, Subraelu P (2007) Coastal Topography and Tsunami Impact: GIS/GPS-based Mobile Mapping of the coastal sectors affected by 2004-tsunami in Krishna–Godavari delta region. East Geogr 13:67–74

Nageswara Rao K, Subraelu P, Rajawat AS, Ajai (2008) Beach erosion in Visakhapatnam: causes and remedies. East Geogr 14:1–8

Nayak SR, Sarangi RK, Rajawat AS (2001) Application of IRS-P4 OCM data to study the impact of cyclone on coastal environment of Orissa. Curr Sci 80:1208–1213

NSIDC (National Snow and Ice Data Center) (2007) Arctic sea ice news Fall 2007. Available via http://nsidc.org/news/Press/2007_seaice minimum/20070810_index.html. Accessed on 29 July 2008

Parry M, Palutikof J, Hanson C, Lowe J (2008) Squaring up to reality. Nature Reports climate change. 2:68 doi:10.1038/climate.2008.50

Pendleton EA, Thieler ER, Williams SJ (2004) Coastal vulnerability assessment of Cape Hettaras National Seashore (CAHA) to sea level rise. USGS Open File Report 2004-1064. Available from http://pubs.usgs.gov/of/2004/1064/images/pdf/caha.pdf accessed on 30 Aug 2008

Pielke RA Jr (2008) Climate predictions and observations. Nat Geosci 1:206 doi:10.1038/ngeo157

Pielke RA Jr, Prins G, Rayner S, Sarewitz D (2007) Lifting the taboo on adaption. Nature 445:597–598 doi:10.1038/445597a

Pielke RA Jr, Wigley T, Green C (2008) Dangerous assumptions. Nature 452:531–532 doi:10.1038/452531a

Pirazzoli PA (1996) Sea-level changes: the last 20,000 years, Wiley, Chichester

Pye K, Blott SJ (2006) Coastal processes and morphological change in the Dunwich—Sizewell area, Suffolk, UK. J Coast Res 22:453–473 doi:10.2112/05-0603.1

Ramanamurthy MV, Sundaramoorthy S, Pari Y et al (2005) Inundation of seawater in Andaman and Nicobar islands and parts of Tamil Nadu coast during 2004 Sumatra tsunami. Curr Sci 88:1736–1740

Rignot E, Bamber JL, van der Broeke MR et al (2008) Recent Antarctic ice mass loss from radar interferometry and regional climate modeling. Nat Geosci 1:106–110 doi:10.1038/ngeo102

Rosenzweig C, Koroly D, Vicarelli M et al (2008) Attributing physical and biological impacts to anthropogenic climate change. Nature 453:353–357 doi:10.1038/nature06937

Sanchez-Arcilla A, Jimenez A, Valdemoro HI (1998) The Ebro delta: morphodynamics and vulnerability. J Coast Res 14:754–772

Schiermeier Q (2008) What we don't know about climate change. Nature 445:580–581

Stroeve J, Holland MM, Meier W et al (2007) Arctic sea ice decline: faster than forecast. Geophys Res Lett 34:L09501 doi:10.1029/2007GL029703

Strohecker K (2008) World sea levels to rise 1.5 m by 2100: scientists, an Environmental News Network and Reuters publication. Available via http://www.enn.com/wildlife/article/34702. Accessed on 24 July 2008

Tanh PTT, Furukawa M (2007) Impact of sea level rise on coastal zone of Vietnam. Bull Fac Sci Univ Ryukyus 84:45–59

Thieler ER, Hammer-Klose ES (1999) National assessment of coastal vulnerability to sea level rise: preliminary results for the U.S. Atlanta coast. USGS, Open File Report 99-593. Available via http://pubs.usgs.gov/of/1999/of99-593/index.html Accessed on 30 Aug 2008

Thompson DWJ, Kennedy JJ, Wallace JM, Jones PD (2008) A large discontinuity in the mid-twentieth century in observed global-mean surface temperature. Nature 453:646–649 doi:10.1038/nature06982

Trenberth KE, Jones PD, Ambenje P et al (2007) Observations: surface and atmospheric climate change. In: Solomon S, Qin D, Manning M et al (eds) Climate Change 2007. The physical science basis. Contribution of WG 1 to the Fourth Assessment Report of the Intergovernmental Panel on Climate Change Cambridge University Press, Cambridge, pp pp 235–336

Unnikrishnan AS, Rup Kumar K, Fernandes SE et al (2006) Sea level changes along the Indian coast: observations and projections. Curr Sci 90:362–368

Unnikrishnan AS, Shankar D (2007) Are sea-level-rise trends along the coasts of the north Indian Ocean consistent with global estimates? Global Planet Change 57:301–307 doi:10.1016/j.gloplacha.2006.11.029

Vethamony P, Sudheesh K, Rupali SP et al (2006) Wave modeling for the north Indian Ocean using MSMR analysed winds. Int J Remote Sens 27:3767–3780 doi:10.1080/01431160600675820

Wood R (2008) Natural ups and downs. Nature 453:43–45 doi:10.1038/453043a

Wu S, Yarnal B, Fisher A (2002) Vulnerability of coastal communities to sea-level rise: a case study of Cape May County, New Jersey, USA. Clim Res 22:255–270 doi:10.3354/cr022255

Zwiers F, Hegerl G (2008) Attributing cause and effect. Nature 453:296–297 doi:10.1038/453296a